Modelling Simul. Mater. Sci. Eng. 1 (1993) 361–372. Printed in the UK

Simulation of electrons solvated in molten salt: a discretized path integral molecular dynamics study with quantum indistinguishability at high temperature

V Iyer†, G E Jabbour†, P A Deymier† and C Y Lee‡

†Department of Materials Science and Engineering, University of Arizona, Tucson, AZ 85721, USA

‡Electronics and Telecommunications Research Institute, Tae Dok Dan Ji, Taejon, Korea

Received 22 June 1992, accepted for publication 9 September 1992

Abstract. We present the use of discretized path integral molecular dynamics in simulating two electrons solvated in molten KCl at high temperatures. In this approach, we use an exact effective potential to simulate the singlet state (antiparallel spins), whereas we introduce an approximate effective potential for the triplet state (parallel spins). The paths for the triplet state are restricted to the region of phase space with positive density matrix. The convergence of the algorithm is presented along with the nature of the electronic states. We then discuss the validity of the introduced effective potentials by comparing our results to those obtained by another quantum molecular dynamics method which uses direct integration of the time-dependent Schrödinger equation. For this high-temperature test problem, the results come to an excellent agreement with those of previous studies.

1. Introduction

Quantum path integral (QPI) is a standard method to study quantum many-body systems. In the discretized path integral representation, an isomorphism between a quantum and a classical system can be exploited to investigate complex quantum systems at finite temperatures [1].

Monte Carlo path integral methods have been used to calculate the properties of many-body bosonic [2] and fermionic [3] systems. Quantum exchange is accounted for in these computations by considering permutations of particles. In cases involving Fermi statistics, there exist permutation cycles with negative weights which lead to difficulties in convergence; especially at low temperatures.

On the other hand, the discretized version of the path integral method in conjunction with the molecular dynamics (MD) technique has been employed to simulate a single electron solvated in a very dilute liquid halide solution, namely KCl [4]. In this work, localization of the electron in a cavity surrounded by cations corroborated experimental findings of an F-center-like state. Albeit simple, the discretized path integral suffers serious limitations with regards to quantum indistinguishability and calculation of the dynamical properties of quantum particles [5].

To alleviate these limitations, Selloni *et al* [6] have tackled the problem of excess electrons solvated in molten KCl by simultaneously solving the time-dependent Schrödinger equation for the excess electrons and the classical equations of motion

0965-0393/93/040361+12$07.50

for the ions. The exchange was included within the local spin density approximation. Their model is constructed within the adiabatic approximation.

Here we introduce a method for incorporating quantum indistinguishability in path integral molecular dynamics (PIMD). In section 2, we deal with the formulation of the partition function for a two-electron system. We discuss the concept of effective potentials which allow for quantum exchange in a classical Lagrangian. The effective potential is exactly defined for two electrons with antiparallel spins. However, for electrons with parallel spins, an approximate effective potential is introduced to avoid the difficulties arising from the antisymmetric property of the density matrix. This effective potential constrains the paths to regions of phase space with positive density matrix. This approximate effective potential is justified on the basis of high temperature and the asymmetry in the quantum paths of indistinguishable electrons resulting from the Coulomb repulsion. We study a test system which is composed of two electrons with various spin states in a non-stoichiometric molten KCl salt. This system was chosen mainly for comparison to the work of Selloni *et al*, who employed it in their simulations. Our results show that the basis for the approximate effective potential used in this paper in the case of the parallel spin (triplet state) is well founded. In agreement with previous studies, the triplet state electrons form two dissociated polarons. On the other hand, the antiparallel spin electrons are observed to evolve toward a localized bipolaronic complex.

The electronic energies obtained are found to be in excellent accord to those calculated by Selloni *et al*. This asserts the effectiveness of the exchange potential we use in the PIMD as a powerful means of simulating many-body systems of indistinguishable particles at high temperatures.

Conclusions are drawn in section 3, including remarks on the limitations of the method.

2. Two-electron systems

2.1. Method

The quantum N-body partition function, with periodic boundaries and in an external potential, may be written in the form [7]

$$Q_P = \left(\frac{1}{N!}\right)^P \left[\frac{Pm}{2\hbar^2\beta}\right]^{3NP/2} \int \prod_{j=1}^{N}\prod_{i=1}^{P} \mathrm{d}r_i^{(j)} \prod_{k=1}^{P} M[A_{k,k+1}]$$
$$\times \exp\left(-\frac{\beta}{P}\sum_{j=1}^{N}\sum_{i=1}^{P}\phi(r_i^{(j)})\right) \exp\left(-\frac{\beta}{P}\sum_{j>l}^{N}\sum_{i=1}^{P}\psi_{jl}(r_i^{(j)} - r_i^{(l)})\right) \qquad (1)$$

where $[A_{k,k+1}]$ is an $N \times N$ matrix whose components are given in the high-temperature limit by

$$A_{k,k+1}^{\alpha\beta} = \exp\left(-\beta\frac{C}{2}(r_k^{(\alpha)} - r_{k+1}^{(\beta)})^2\right) \qquad \alpha,\beta = 1,2,\ldots,N \qquad (2)$$

where $C = Pm/\hbar^2\beta^2$.

In the above equation for the partition function; $\phi(r_i^{(j)})$ refers to the external potential, and the extra term $\psi_{jl}(r)$ is the Coulombic interaction between the quantum par-

ticles j and l. In the absence of quantum exchange,

$$M[A_{k,k+1}] = \prod_{\alpha=1}^{N} A_{k,k+1}^{\alpha\alpha}$$

each electron is represented by a closed 'polymeric' necklace containing P nodes with cyclic condition $r_p^{(\alpha)} - r_{p+1}^{(\alpha)} = r_p^{(\alpha)} - r_1^{(\alpha)}$. Quantum indistinguishability (exchange) leads to a complex $(N \times P)$-body problem where linkage between the N cyclic 'polymeric' necklaces to form dimers, trimers, etc occurs. For a two-electron system,

$$M[A_{k,k+1}] = \det_{\text{perm}} [A_{k,k+1}] = \exp\left(-\beta(C/2)[(r_k^{(1)} - r_{k+1}^{(1)})^2 + (r_k^{(2)} - r_{k+1}^{(2)})^2]\right)$$
$$+ \zeta \exp\left(-\beta(C/2)[(r_k^{(1)} - r_{k+1}^{(2)})^2 + (r_k^{(2)} - r_{k+1}^{(1)})^2]\right). \quad (3)$$

M represents a determinant or a permanent when the exchange parameter ζ takes values $+1$ or -1. $\zeta = +1$ corresponds to a symmetric orbital part of the two-electron wave function (total spin $S = 0$, or singlet state). $\zeta = -1$ corresponds to an antisymmetric orbital wave function with spin state $S = 1$ (triplet state).

The first term in equation (3) represents the two electrons in the absence of exchange whereas the second term consists of an exchange contribution.

2.1.1. Electrons with antiparallel spins $\{\zeta = +1\}$. $M[A_{k,k+1}] = \text{perm}\,[A_{k,k+1}]$ is positive for all states. We can therefore define $\text{perm}\,[A_{k,k+1}] = \exp(-\beta V_{\text{eff}})$ where we introduce an exact effective potential in the form

$$V_{\text{eff}} = \tfrac{1}{2} C(r_k^{(1)} - r_{k+1}^{(1)})^2 + \tfrac{1}{2} C(r_k^{(2)} - r_{k+1}^{(2)})^2$$
$$- (1/\beta) \ln\{1 + \exp[-\beta C(r_k^{(1)} - r_k^{(2)}) \cdot (r_{k+1}^{(1)} - r_{k+1}^{(2)})]\}. \quad (4)$$

We have used the relation

$$2(r_k^{(1)} - r_k^{(2)}) \cdot (r_{k+1}^{(1)} - r_{k+1}^{(2)}) = (r_k^{(1)} - r_{k+1}^{(2)})^2 + (r_k^{(2)} - r_{k+1}^{(1)})^2$$
$$- (r_k^{(1)} - r_{k+1}^{(1)})^2 - (r_k^{(2)} - r_{k+1}^{(2)})^2. \quad (5)$$

The last term in equation (4) is an exchange contribution to the effective potential and can be very easily incorporated in a classical MD algorithm.

It is instructive to calculate the effective force on the electron (1) in state 'k' arising from the effective potential function given in equation (4).

$$F_k^{(1)} = -\partial V_{\text{eff}} / \partial r_k^{(1)} = -C[f \cdot (r_k^{(1)} - r_{k+1}^{(1)}) + (1 - f) \cdot (r_k^{(1)} - r_{k+1}^{(2)})] \quad (6)$$

where

$$f = f(r_k^{(1)}, r_k^{(2)}, r_{k+1}^{(1)}, r_{k+1}^{(2)}) = \frac{1}{1 + \exp[-\beta C(r_k^{(1)} - r_k^{(2)}) \cdot (r_{k+1}^{(1)} - r_{k+1}^{(2)})]}. \quad (7)$$

We may write $F_k^{(1)} = F_{(1)(1)} + F_{(1)(2)}$ where the subscripts (1)(1) and (1)(2) stand for the two possible events for electron (1) in state k; namely (a) annihilation of electron (1) in state k and creation of electron (1) in state $k+1$ and (b) annihilation of electron (1) in state k and creation of electron (2) in state $k+1$, respectively. In the singlet state $(\zeta = +1)$, the function f behaves like a Fermi function. f and $(1-f)$ are positive. Attractive effective forces, $F_{(1)(1)}$ and $F_{(1)(2)}$, act between the states k and $k+1$ of electron (1), and k of electron (1) and $k+1$ of electron (2), respectively.

The value of the function 'f' depends on the topology of the k and $k+1$ states of both electrons. The function 'f' weights the two events (a) and (b). Clearly, symmetrical effective forces apply on electrons (1) and (2) in states k and $k+1$.

2.1.2. Electrons with parallel spins $\{\zeta = -1\}$. For the parallel spins case, $M[A_{k,k+1}]$ takes the form of a determinant

$$\det[A_{k,k+1}] = \exp\left(-\beta(C/2)[(r_k^{(1)} - r_{k+1}^{(2)})^2 + (r_k^{(2)} - r_{k+1}^{(2)})^2]\right)$$
$$\times \{1 - \exp[-\beta C(r_k^{(1)} - r_k^{(2)}) \cdot (r_{k+1}^{(1)} - r_{k+1}^{(2)})]\}. \tag{8}$$

In this case, the difficulty in defining an effective potential resides in the fact that the partition function is a sum over terms which can be either positive or negative. In order to produce an effective classical potential useful in a computer simulation, one would like to rewrite the partition function in a way that corresponds to a sum of positive terms.

Monte Carlo simulations of a two-dimensional non-interacting system constituting of two polarized fermions in a harmonic potential have been reported [8]. In this study, two sampling methods were used, namely the usual importance sampling of particle permutation and coordinates and a sampling based on weight functions including explicitly the determinant, $\det[A_{k,k+1}]$. Both weight functions can take negative values; however the fraction of states with negative signs sampled by the determinant method is much smaller. At high temperatures, the ratio of negative signs becomes very small. At fixed PT, this fraction increases with decreasing temperature to 50%.

Recent path-integral calculations of a fermion system of liquid ^{3}He atoms in the normal state indicate that a restriction of the paths to a region of phase space with a positive density matrix gives reasonable results at relatively high temperatures above 1 K [9]. Considering the heavy mass of ^{3}He atoms, 1 K falls in the high-temperature region. These two studies suggest that under conditions of high temperature, we can restrict phase space to a region of positive determinant and define an approximate effective potential in the form

$$V_{\text{eff}} = \tfrac{1}{2}C(r_k^{(1)} - r_{k+1}^{(1)})^2 + \tfrac{1}{2}C(r_k^{(2)} - r_{k+1}^{(2)})^2$$
$$- (1/\beta)\ln\{1 - \exp[-\beta C(r_k^{(1)} - r_k^{(2)}) \cdot (r_{k+1}^{(1)} - r_{k+1}^{(2)})]\} \tag{9a}$$
$$\text{if} \quad (r_k^{(1)} - r_k^{(2)}) \cdot (r_{k+1}^{(1)} - r_{k+1}^{(2)}) > 0$$

and

$$V_{\text{eff}} = \tfrac{1}{2}C(r_k^{(1)} - r_{k+1}^{(1)})^2 + \tfrac{1}{2}C(r_k^{(2)} - r_{k+1}^{(2)})^2 \tag{9b}$$
$$\text{if} \quad (r_k^{(1)} - r_k^{(2)}) \cdot (r_{k+1}^{(1)} - r_{k+1}^{(2)}) \leq 0.$$

In the case of interacting fermions, the Coulombic repulsion between the electrons dictates the distance between nodes in their respective necklaces. The distance between two successive nodes within a necklace decreases as the number of nodes P increases. At high effective temperature PT that is high temperature and/or large number of nodes P), the large classical force constant C imposes $|r_k^{(1)} - r_k^{(2)}|$ and $|r_{k+1}^{(1)} - r_{k+1}^{(2)}|$ to be greater than $|r_{k_{+1}}^{(1)} - r_{k+1}^{(1)}|$ and $|r_k^{(2)} - r_{k+1}^{(2)}|$ leading to a topological constraint on the sign of $(r_k^{(1)} - r_k^{(2)}) \cdot (r_{k+1}^{(1)} - r_{k+1}^{(2)})$. In other words,

under these conditions, the Coulombic interaction breaks the symmetry between a path within a necklace and a path between different necklaces. Since the partition function is independent of the number of nodes for sufficiently large values, we may conveniently choose P such that positive determinants are the major contributors to Q.

The effective force on state 'k' of electron (1) takes the form

$$\boldsymbol{F}_k^{(1)} = -C[f\cdot(\boldsymbol{r}_k^{(1)} - \boldsymbol{r}_{k+1}^{(1)}) + (1-f)\cdot(\boldsymbol{r}_k^{(1)} - \boldsymbol{r}_{k+1}^{(2)})] \tag{10}$$

where

$$f = \frac{1}{1 - \exp[-\beta C(\boldsymbol{r}_k^{(1)} - \boldsymbol{r}_k^{(2)})\cdot(\boldsymbol{r}_{k+1}^{(1)} - \boldsymbol{r}_{k+1}^{(2)})]}$$

$$\text{if} \quad (\boldsymbol{r}_k^{(1)} - \boldsymbol{r}_k^{(2)})\cdot(\boldsymbol{r}_{k+1}^{(1)} - \boldsymbol{r}_{k+1}^{(2)}) > 0$$

and

$$f = 1 \qquad \text{if} \quad (\boldsymbol{r}_k^{(1)} - \boldsymbol{r}_k^{(2)})\cdot(\boldsymbol{r}_{k+1}^{(1)} - \boldsymbol{r}_{k+1}^{(2)}) \le 0.$$

In the rare event that we attain states for which the determinant is negative, the nature of the force in equation (10) pushes the system towards the positive regime. In general this effective potential will bias the sampling of phase space to the region of positive determinants. However, when employed at high temperatures, this restriction appears to constitute a satisfactory representation of exchange interactions. It will be shown in the results section that indeed the states with negative determinants are extremely rare for the system under investigation at high temperatures.

2.1.3. Optimum number of nodes. The discretized path integral represents the exact quantum system when the number of nodes P tends to infinity. However, there exists a minimum value of P above which the properties of the classical system have nearly converged to the properties of the quantum system. The discretization of the electron is determined by the ratio of the potential energy of the electron to the thermal energy. In the case of an electron solvated in a molten KCl salt, the potential energy is taken as the Coulomb potential of the electron due to a nearby ion. Using a pseudopotential representation of K^+, the maximum potential energy arises when the electron is localized within the core of a K ion, namely $e^2/4\pi\epsilon_0 R_C$ where R_C is the radius of the core. Taking $R_C \simeq 2$ Å [4], the condition $P > e^2/4\pi\epsilon_0 R_C kT$ yields a lower bound for our system of approximately 60 for the number of nodes. This number is in agreement with the calculations of Parrinello and Rahman [4] for a single electron solvated in molten KCl.

Intuitively, there should exist a value for P above which the exchange events will not be computationally tractable. For evaluating this upper limit, we consider exchange between two electrons in the absence of external fields for ease of argument. For a system with P nodes the partition function Q can be split into two terms, namely

$$Q = Q_1 + Q_{\text{exch}} \tag{11}$$

where Q_1 represents the partition function in the absence of exchange and Q_{exch} contains terms arising from all possible combinations of exchanging nodes.

When factoring Q_1, the total partition function becomes

$$Q = Q_1\left(1 + \frac{Q_2}{Q_1} + \frac{Q_3}{Q_1} + \frac{Q_4}{Q_1} + \ldots\right) \tag{12}$$

where $Q_{i>1}$ denotes all possible exchange processes.

In order to set a maximum limit for P we divert our attention to the evaluation of the ratios of partition functions. This can be done using the energy distribution method [10, 11].

Let us consider two systems differing in their potential energies. A reference system $U_{(1)}$ for two electrons in the absence of exchange interactions, namely

$$U_{(1)} = \sum_{(i=1)}^{P*} \frac{C}{2}(r_i^{(1)} - r_{i+1}^{(1)})^2 + \sum_{(i=1)}^{P*} \frac{C}{2}(r_i^{(2)} - r_{i+1}^{(2)})^2 + \sum_{i=1}^{P*} \psi(r_i^{(1)} - r_i^{(2)}) \tag{13}$$

and the system of interest $U_{(2)}$ for two necklaces with some nodes exchanging. For example, for one exchange process at node 'j' the potential reads

$$U_{(2)} = \sum_{\substack{i=1 \\ i\neq j}}^{P*} \frac{C}{2}(r_i^{(1)} - r_{i+1}^{(1)})^2 + \sum_{\substack{i=1 \\ i\neq j}}^{P*} \frac{C}{2}(r_i^{(2)} - r_{i+1}^{(2)})^2 + \frac{C}{2}(r_j^{(1)} - r_{j+1}^{(2)})^2$$

$$+ \frac{C}{2}(r_j^{(2)} - r_{j+1}^{(1)})^2 + \sum_{i=1}^{P*} \psi(r_i^{(1)} - r_i^{(2)}) \tag{14}$$

where Σ^* denotes the cyclic condition on the necklaces.

A two-sided evaluation of the ratio of partition functions between two identical systems experiencing different potentials is based on the construction of two normalized distribution functions $h_1(x)$ and $h_2(x)$, which are given by

$$h_1(x) = \langle \delta(U_1 - U_2 - x) \rangle_1 = \int \delta(U_1 - U_2 - x) \exp\left(-\frac{U_1}{kT}\right) \mathrm{d}\boldsymbol{r}\, \mathrm{d}\boldsymbol{v}/Q_1 \tag{15}$$

$$h_2(x) = \langle \delta(U_1 - U_2 - x) \rangle_2 = \int \delta(U_1 - U_2 - x) \exp\left(-\frac{U_2}{kT}\right) \mathrm{d}\boldsymbol{r}\, \mathrm{d}\boldsymbol{v}/Q_2 \tag{16}$$

where $\langle\ \rangle_1$ and $\langle\ \rangle_2$ refers to the respective ensemble averages and δ is the usual delta function.

The ratio of partition functions is related to the ratio of these distribution functions at some point x, namely

$$\frac{Q_1}{Q_2} = \exp\left(-\frac{x}{kT}\right)\left(\frac{h_2(x)}{h_1(x)}\right). \tag{17}$$

The ratio can be calculated only if there is sufficient overlap of the distributions h_1 and h_2. A simple criterion that evolves for the satisfactory estimation of the ratio of partition functions is that the gap between the distributions be no larger than kT and that the distributions be broader than the gap [10]. The relative magnitude of the energy distribution spread for P particles follows the proportionality

$$\sigma_E/E \propto 1/P^{1/2} \tag{18}$$

where σ_E is the variance of the distribution, and E is the average energy.

The gap between the distributions normalized to the average energy taken as the Coulombic energy is written in the form

$$\text{gap} \propto kT/(e^2/4\pi\epsilon_0 r_i) \tag{19}$$

where r_i is some appropriate length.

Applying the condition for effective overlap, we get

$$e^2/4\pi\epsilon_0 r_i kT > P^{1/2}. \tag{20}$$

Assigning suitable values (r_i is taken as 6.9 Å or the cut-off range in our simulation cell, and $T = 1300$ K), we arrive at an upper bound of the order of 300 for efficient exchange sampling.

2.2. Model

We conducted MD simulations using the QPI approach on a system constituted of two electrons solvated in molten KCl. The states of the system are sampled by trajectories generated by the classical Hamiltonian [4]

$$H = \sum_{i=1}^{P} \tfrac{1}{2} m^* \dot{r}_i^{(1)^2} + \sum_{i=1}^{P} \tfrac{1}{2} m^* \dot{r}_i^{(2)^2} + \sum_{I=1}^{N} \tfrac{1}{2} M_I \dot{R}_I^2 + V_{\text{eff}} + \sum_{I>J} \phi_{IJ}(R_{IJ}) + \sum_{i=1}^{P} \sum_{\gamma>\mu}^{N} \psi_{\gamma\mu}(r_i^\gamma - r_i^\mu) + \sum_{i=1}^{P} \sum_{\gamma=1}^{N} \frac{\phi_\gamma(r_i^\gamma)}{P} \tag{21}$$

where V_{eff} is given by equation (4) when $\zeta = +1$ (the singlet states) or by equation (9) when $\zeta = -1$ (triplet state). The masses M_I are taken as the ionic masses and m^* is an arbitrary mass assigned to each node on the classical 'necklace'. We use one atomic mass unit [4]. The potential $\phi_{IJ}(R_{IJ})$ models the interactions between ions.

The simulation cell is a fixed cubic box with edge length $L = 13.8$ Å, containing 32 K^+ and 30 Cl^- ions. Periodic boundary conditions were subsequently imposed on the system. The interaction between the ions are of the Born–Mayer–Huggins type and we used the parameter of Sangster and Atwood [12]. The electron/K^+ interaction is modelled with a local pseudopotential with a core radius $R_C = 1.96$ Å [4]. Since an electron is already repelled by a chlorine ion, core corrections are not very important. We chose a purely Coulombic potential to model the electron/Cl^- interaction. The long-range Coulombic potential and forces are calculated with the Ewald summation method. All simulations in this study have been performed with the following set of conditions: Ewald parameter $\eta = 5.741/L$, and a real-space part of the summation truncated at $\frac{1}{2}L$. With this choice of parameters the k-space sum in the Ewald construction is small compared to real-space contributions and is neglected [13]. The Coulombic interactions between electrons are calculated using the minimum-image criterion [14]. The equations of motion are solved with a finite difference scheme, and the time integration step is $\Delta t = 2.68 \times 10^{-15}$ s. The temperature is 1300 K. This temperature is chosen for comparison with the work of Selloni *et al.* It is also sufficiently high for the path integral method with exchange introduced in the preceding section to be practical with reasonable values for the number of nodes, P. Temperature is maintained constant by using a momentum rescaling thermostat [15]. We employ one thermostat for the ionic species. Each electronic necklace is in contact with its own individual thermostat. This approach avoids drifts in temperature of the ions due to transfer of energy between the ions and the electrons, thus maintaining adiabaticity [16].

To calculate the energy of a two-electron system, we use the energy estimator

$$\langle E \rangle = 2\left(\frac{3P}{2\beta}\right) - C\left\langle \sum_{k=1}^{P} f[(r_k^{(1)} - r_{k+1}^{(1)})^2 + (r_k^{(2)} - r_{k+1}^{(2)})^2 + (1-f)[(r_k^{(1)} - r_{k+1}^{(2)})^2 + (r_k^{(2)} - r_{k+1}^{(1)})^2 \right\rangle$$

$$+\left\langle \sum_{k=1}^{P} \frac{\psi_{12}(r_k^{(1)} - r_k^{(2)})}{P} \right\rangle + \left\langle \sum_{i=1}^{2} \sum_{k=1}^{P} \frac{\phi(r_k^{(i)})}{P} \right\rangle \tag{22}$$

where f was defined in equation (7) for $\zeta = +1$ and in equation (10) for $\zeta = -1$.

In this paper, the last two terms in equation (22) are referred to as the Coulombic energy (Hartree energy) and potential energy (electron/ion energy).

The estimator for the kinetic energy possesses some numerical drawbacks. It is a difference between two large quantities (growing with the number of nodes, P) and its variance increases also with P [4]. A better estimator for the kinetic energy derived by Herman *et al* [17] in the form of a virial is not usable in our case of two exchanging electrons. The virial estimator applies only to a partition function which is homogeneous and of degree two. On examination of equation (1), it is clear that this condition is not satisfied for $\zeta = +1$ and $\zeta = -1$. Large uncertainties in the value for the kinetic energy calculated from the first two terms of equation (22) are therefore expected; particularly for large numbers of nodes.

2.3. *Results and discussion*

2.3.1. Convergence of algorithm. The effect of time steps on our simulations was tested. Three sets of runs were conducted with time steps, Δt, $\Delta t/2$, $\Delta t/4$. Analysis indicated negligible variance with decreasing time steps. We therefore chose the largest Δt for all subsequent simulations.

Table 1 shows a comparison of energies for $\zeta = 0, +1, -1$ with variable node specifications of 10, 50, 100, 176 and 288. The standard deviations for the Coulombic, potential and kinetic energies were of the order of 0.3, 0.8 and 2.0 eV respectively. The large deviations in the kinetic energies arise from the use of equation (22). It should be noted that the standard deviations do not represent the errors made on averaging a finite set of energies, but instead represent the spread of the instantaneous energies.

The singlet state ($\zeta = +1$) exhibits an unreasonably small value of the Coulombic energy for $P = 10$ nodes. However, for P in the interval 50–288 nodes, all the values of the Coulombic and potential energies are within the range dictated by their respective standard deviations. As P tends to values greater than 300 nodes we predicted that the exchange interactions, though present, would not be fully sampled. We should thus expect a gradual convergence to the $\zeta = 0$ state as $P \to \infty$. We have not been able to simulate systems larger than 300 nodes due to computational limitations. However, our numerical calculations for $\zeta = +1$ indicate clearly that the path integral method with exchange has converged for $P \geqslant 50$ nodes at the temperature 1300 K.

The $\zeta = 0$ system constantly fluctuates between the singlet and triplet states. Averaging out values requires very long simulations. It appears that, for P greater than 100, the energies have converged. In this case, since no exchange interaction is taking place, large values of P do not limit the simulation. In fact accurate values of energies can be obtained by increasing P.

For the $\zeta = -1$ (triplet) case, we specified the need for the exchange sampling to be limited to states with positive sign. A simple criterion for the topological constraint to hold is that the exchange distances exceed the harmonic distances. The minimum exchange distance is determined by the Coulomb repulsion between the electrons. We estimate a lower limit for our model of $2R_C \simeq 4$ Å. This limit corresponds to two elec-

Table 1. Comparison of energies for $\zeta = 0, +1, -1$ with variable number of nodes. The energies are referred to a state of zero energy for infinitely separated particles. Energies are in eV. The standard deviations for the Coulombic, potential and kinetic energies are of the order of 0.3, 0.8 and 2.0 eV, respectively.

Nodes	Coulombic	Potential	Kinetic	Timesteps
$\zeta = 0$				
10	4.0	−20.36	1.4	100 000
50	3.8	−16.1	1.3	30 000
100	3.7	−15.5	1.7	25 000
176	4.0	−16.5	2.1	100 000
288	4.0	−14.9	2.1	100 000
$\zeta = +1$				
10	3.9	−19.8	1.1	100 000
50	4.6	−19.5	1.8	30 000
100	4.7	−18.7	1.8	25 000
176	4.5	−17.9	2.2	100 000
288	4.6	−18.7	2.2	100 000
$\zeta = -1$				
10	3.1	−19.6	1.2	100 000
50	3.5	−16.6	2.2	30 000
100	3.6	−16.2	2.2	25 000
176	3.7	−16.2	2.0	100 000
288	3.5	−14.1	2.1	100 000

trons trapped in the core of a single potassium ion. The topological constraint is verified if on the average the harmonic distance, $\bar{d}_{\text{harm}}$, is less than 4 Å. Let us take 1 Å as a sufficiently lower value. The average harmonic energy can be written in the form

$$\frac{1}{2}\frac{Pm}{\hbar^2 B^2}\left(\sum_{i=1}^{P}{}^{*}\,\bar{d}^2_{\text{harm}}\right) = \frac{1}{2}\frac{Pm}{\hbar^2\beta^2}(P\bar{d}^2_{\text{harm}}).$$

This energy is of the order of $\frac{3}{2}P/\beta$ leading to the relation $PT = 3\hbar^2/mk\bar{d}^2_{\text{harm}}$. Inserting the appropriate values gives $PT \simeq 24 \times 10^4$ as a high enough effective temperature. Theoretical values for P above 100 at $T = 1300$ K appear to be suitable by effectively restricting the phase space for exchange interaction. We also note that for all temperatures, the number of nodes for the topological constraint to hold lies below the maximum of P for efficient exchange sampling and above the minimum value for convergence of the classical isomorphism. Therefore, there exists an interval for P in which all conditions are satisfied.

We conducted simulations of the parallel spin electrons ($\zeta = -1$) with the main objective of monitoring the frequency of occurrence of states with negative determinants. In view of the random initial configuration used, we noted that for systems with $P \simeq 100$, in the initial stage of the simulations (~5000 steps), there were a few exchange processes which entered the negative regime with a frequency of approximately 300 steps. Thereafter, once equilibrium was reached these transgressions decreased rapidly to a maximum rate of one negative exchange every 20 000 steps. We also noted, as predicted, that the probability of these states decreased further with increasing number of nodes in simulations of larger systems. For $P = 10$ nodes, we are far below the boundary limits of the approximate effective potential. For P values of 50–288, we obtain fairly convergent values of energies. As P tends to larger numbers, as stated earlier, we anticipate a problem of ineffective sampling of the states.

Table 2. Energies (eV) for a single electron and two-electron systems with parallel and antiparallel spins solvated in molten KCl ($P = 100$) referred to a state of zero energy for infinitely separated particles. The numbers in parentheses are standard deviations.

	Path integral		
	$\zeta = +1$	$\zeta = -1$	One electron
Kinetic energy	1.8(1.4)	2.2(2)	1.2(0.3)
Coulombic energy	4.7(0.3)	3.6(0.4)	—
Potential energy	−18.7(0.8)	−16.2(0.6)	−8.3(0.5)

In summary, in all three cases, $\zeta = +1, 0, -1$, satisfactory thermodynamic properties are seen to be obtained in the range of 50 to 300 nodes.

2.3.2. Nature of electronic states. Table 2 compares the energy of a single electron immersed in a 32 K^+ and 31 Cl^- molten salt to that of two-electron systems. We chose the 100-node system for simple illustrative purposes. For the sake of comparison, the energies are referred to a state of zero energy for infinitely separated particles. By a simple analysis it can be seen that the potential energy of the single electron is approximately half the energy of the triplet ($\zeta = -1$) state. This clearly indicates the retention of two dissociated polaronic states. On the other hand, the singlet ($\zeta = +1/S = 0$) state shows a lower potential energy.

The Coulombic energy term shows a higher value for the singlet state than the triplet configuration. The increase in electron–electron Coulombic energy for the singlet state is offset by a decrease in its potential energy. Electrons with parallel spin feel a negligible part of the short-range Coulombic repulsion, as they are kept apart by Pauli's exclusion principle. Only electrons of antiparallel spins interact via the large-momentum-transfer part of the Coulomb interaction, namely at small separation distances. The singlet state is more commonly referred to as a bipolaronic complex.

These observations are substantially corroborated by the electronic configurational plots and electron pair radial distributions. Figure 1 shows the singlet and triplet radial distributions. For the $\zeta = +1$ case we see that a bipolaronic complex is formed with an

Table 3. Coulombic, potential and kinetic energies (eV) calculated by PIMD versus those reported by Selloni *et al* [6]. The energies are presented in eV. The zero of energy is such that the electron–electron Coulomb energy and the electron–ion potential energy are zero for two uniformly spread electrons. The potential energy of Selloni *et al* is taken as the sum of an exchange and potential energy.

Nodes	Coulombic	Potential	Kinetic
$\zeta = +1 (s = 0)$			
50	3.0(0.3)	−15.7(0.9)	1.8(2.0)
100	3.0(0.3)	−15.3(0.8)	1.8(2.1)
176	2.9(0.3)	−14.1(0.8)	2.2(2.0)
288	3.0(0.3)	−15.1(0.8)	2.2(2.0)
Selloni	3.3(0.2)	−13.3(0.6)	2.3(0.1)
$\zeta = -1 (s = 1)$			
50	1.9(0.4)	−12.8(0.6)	2.2(2.0)
100	2.0(0.4)	−12.4(0.6)	2.2(2.0)
176	2.1(0.4)	−12.4(0.6)	2.0(2.0)
288	1.8(0.4)	−10.3(0.7)	2.1(2.0)
Selloni	2.0(0.5)	−11.1(1.5)	2.9(0.3)

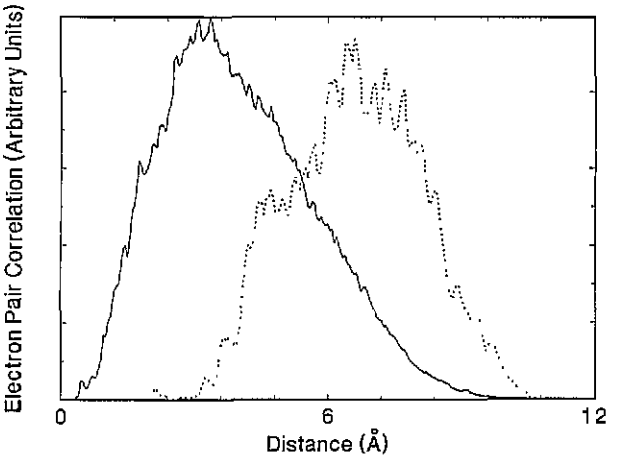

Figure 1. Electron–electron pair correlation functions. The full and broken curves refer to $\zeta = +1$ and $\zeta = -1$, respectively. The radial axis is in Å. We used a radial mesh of 0.05 Å.

average distance between the electrons of ~3.2 Å. In contrast, the electrons with identical spins sit at an average distance of ~7 Å.

2.3.3. Comparison with other quantum MD *approaches.* The energies calculated by the PIMD formalism are compared to those reported by Selloni *et al* [6]. Table 3 summarizes the results obtained in our work for the two-electron system for various numbers of nodes.

The kinetic and potential energies compare qualitatively with our values but cannot be compared quantitatively because of differences in interparticle potentials. Selloni *et al* [5] used a Born–Mayer type potential for the ion–ion interaction with parameters fixed by Fumi and Tosi [18]. The electron–ion potential we used was a truncated pseudopotential [4] whereas Selloni *et al* employed a smoothed version of the same potential.

On the other hand, the electron–electron Coulombic energies are in excellent quantitative agreement. These values are truly representative of the singlet and triplet states. It therefore appears that the PIMD method with quantum exchange at high temperatures produces results comparable to those obtained within the adiabatic and local spin density approximations in Selloni's quantum MD, thus testifying to the quality of both calculations.

3. Conclusion

We have shown that two-electron systems can be simulated with the method of discretized quantum path integral molecular dynamics at high temperatures. In our formalism, exchange between the quantum particles is accounted for through topological effective potentials. The exchange potential for heterospin electrons is exact over a wide range of temperatures unlike the isospin case where it is approximate and justified on the basis of high temperature.

The two test systems investigated, namely two electrons with antiparallel spins, and two electrons with parallel spins solvated in molten KCl, sample the exchanging states effectively. The unpolarized and polarized two-electron systems form an associated bipolaronic complex and two dissociated polaronic states, respectively. We have compared results obtained in our simulations with another quantum molecular dynamics

approach which employs a direct integration of the time-dependent Schrödinger equation. The excellent agreement between the two methods demonstrates that our approach can successfully describe the physics of quantum many-body systems at high temperatures. In contrast to the method of Selloni *et al* which requires a very small integration step ($\sim 10^{-17}$ s) to maintain adiabaticity, the fictitious dynamics in the DPIMD necessitates only a step of the order of 10^{-15} s. The use of the discretized path integral method is, however, limited to the calculation of thermal equilibrium averages and does not provide direct information on the dynamics of the electrons. This problem may be alleviated by using analytical continuation [19, 20], although it suffers from severe statistical errors [21]. In the case of non-polarized electrons, another disadvantage of the method is that simulations at lower temperatures than those used in this paper require larger numbers of necklace nodes. The larger values of P are needed to insure convergence of the discretized path integral but may lead to inefficient sampling of exchanging states. This problem may be overcome to some degree by employing a higher-order correction to the Trotter expansion [22, 23] to reduce the number of nodes for convergence. For isospin fermions, the approximate effective potential is limited to high temperatures. Another drawback of the discretized path integral method is the difficulty in using non-local pseudopotentials [24]. Despite these limitations, the method has the advantage of simplicity and ease of implementation with an ordinary MD scheme. It provides a simple classical description of complex quantum systems of indistinguishable particles at high temperatures.

References

[1] Barker J A 1974 *J. Chem. Phys.* **70** 2914–21
[2] Ceperley D M and Pollock E L 1986 *Phys. Rev. Lett.* **56** 474–7
[3] Broughton J and Abraham F 1988 *J. Phys. Chem.* **92** 3274–7
[4] Parrinello M and Rahman A 1984 *J. Chem. Phys.* **80** 860–7
[5] Selloni A, Fois E S, Parrinello M and Car R 1989 *Phys. Scr.* **725** 261–7
[6] Selloni A, Carnevali P, Car R and Parrinello M 1987 *Phys. Rev. Lett.* **59** 823–6
[7] Chandler D and Wolynes P G 1981 *J. Chem. Phys.* **74** 4078–95
[8] Takahashi M and Imada N 1984 *J. Phys. Soc. Japan* **53** 963–74
[9] Ceperley D M 1992 *Phys. Rev. Lett.* **69** 331
[10] Valleau J P and Torrie G M 1976 *Modern Theoretical Chemistry* vol 5, ed B J Berne (New York: Plenum)
[11] Bennett C H 1976 *J. Comput. Phys.* **22** 245
[12] Sangster M J L and Atwood R M 1978 *J. Phys. Chem.* C **11** 1541
[13] Linse P and Andersen H C 1986 *J. Chem. Phys.* **85** 3027
[14] Wood W W 1968 *Physics of Simple Liquids* ed H N V Temperley, J S Rowlison and G S Rushbrooke (Amsterdam: North-Holland)
[15] Woodcock L V 1971 *Chem. Phys. Lett.* **10** 257
[16] Galli G and Parrinello M 1991 *Computer Simulation in Materials Science* (*NATO ASI Series E: Applied Sciences*) vol 205, ed M Meyer and V Pontikis (Dordrecht: Kluwer) p 283
[17] Herman M F, Bruskin E J and Berne B J 1982 *J. Chem. Phys.* **76** 5150–5
[18] Fumi F G and Tosi M P 1964 *J. Phys. Chem. Solids* **25** 45
[19] Thiramalai D and Berne B J 1983 *J. Chem. Phys.* **79** 5029
[20] Nichols A L and Chandler D 1987 *J. Chem. Phys.* **87** 6671
[21] Malescio G 1987 *Phys. Rev.* A **36** 5847
[22] Takahashi M and Imada M 1984 *J. Phys. Soc. Japan* **53** 3765
[23] Li X P and Broughton J Q 1987 *J. Chem. Phys.* **86** 5094
[24] Ceperley D M 1991 *Computer Simulation in Materials Science* (*NATO ASI Series E: Applied Sciences*) vol 205, ed M Meyer and V Pontikis (Dordrecht: Kluwer) p 321